Experimental study of bed load transport on steep slopes with a two-size mixture of spherical particles

Virginie Hergault
Cemagref Grenoble, ETNA, BP 76, 38402 Saint Martin d'Hères Cedex, France, virginie.hergault@cemagref.fr

Philippe Frey
Cemagref Grenoble , ETNA, BP 76, 38402 Saint Martin d'Hères Cedex, France, philippe.frey@cemagref.fr

Francois Métivier
LDSG IPGP/Paris VII UMR CNRS 7579, France, metivier@ipgp.jussieu.fr

Christophe Ducottet
Laboratoire TSI UMR CNRS 551, 42000 Saint-Etienne, France, ducottet@univ-st-etienne.fr

Tobias Böhm
Cemagref Grenoble, ETNA, BP 76, 38402 Saint Martin d'Hères Cedex, France, tobias.boehm.1976@web.de

Christophe Ancey
Ecole Polytechnique Fédérale de Lausanne, Ecublens, 1015 Lausanne, Switzerland, christophe.ancey@epfl.ch

Bed load transport is a longstanding problem despite its major implication in river morphodynamics. The physical processes ruling coarse-particle/fluid systems are indeed poorly known, impairing our ability to compute local and even bulk quantities such as the sediment flux in rivers. We present an experimental study of a two-size mixture of coarse spherical glass beads entrained by a shallow turbulent water flow down a steep channel with a mobile bed. The particle diameters were 4 and 6 mm, the channel width 6.5 mm and the channel inclination 12.5%. The water flow rate and the solid discharge were kept constant at the upstream entrance. They were adjusted to obtain bed load equilibrium, that is, neither bed degradation nor aggradation over sufficiently long time intervals. Flows were filmed from the side by a high-speed camera. Using image processing algorithms made it possible to determine the position, velocity and trajectory of each spherical particle thanks to a PTV algorithm (particle tracking velocimetry). Transitions of the state of motion (rest, rolling or saltating) and flow depth were also determined. New data were compared to previous results obtained with spherical particles of uniform size. They confirm that the free surface acting as a physical barrier by truncating the saltation trajectories is very important on steep slopes. The use of a two-size mixture with the 4 mm beads tending to be blocked in the 6.5 mm wide channel resulted in a bed mainly formed by these 4 mm beads. This particular structure explained the single peak vertical distribution of the solid discharge contrary to the uniform case where several peaks corresponding to rolling were observed.

1 INTRODUCTION

Despite substantial progress made over the last two decades in the physical understanding of the motion of coarse particles in a turbulent stream, the ability to compute bulk quantities such as the sediment flux in rivers remains poor. For instance, the sediment flow rates measured in gravel-bed rivers differ within one to two orders of magnitude from the bed-load transport equations (Wilcock 2001; Martin 2003; Barry et al. 2004). In order to better understand the physical processes ruling bed-load solid transport at the grain scale, an experimental study of the motion of coarse

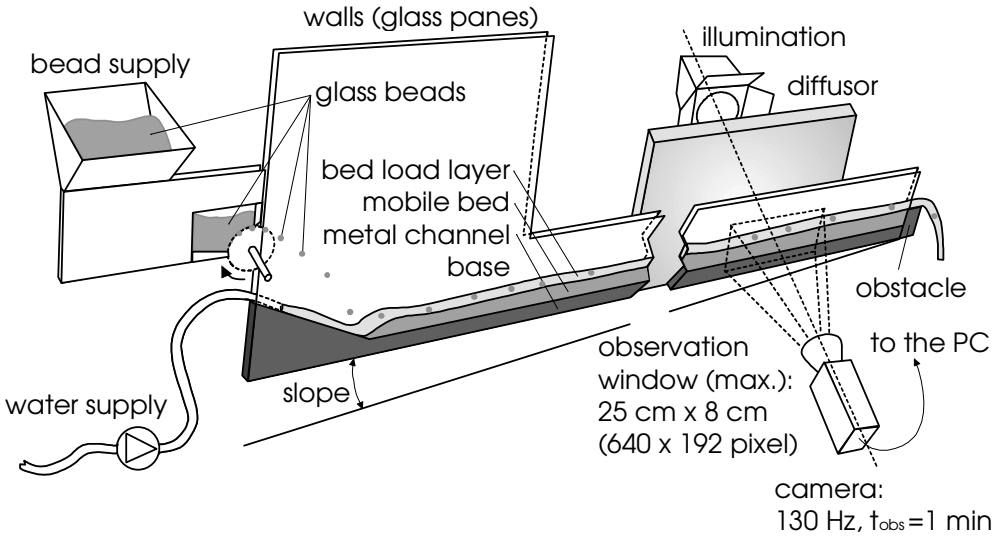

Figure 1: Sketch of the experimental setup (Boehm et al. 2006).

spherical glass beads entrained by a turbulent and supercritical water flow down a steep channel with a mobile bed was set up. The width was 6.5 mm slightly larger than the particle diameter of 6 mm to create a two-dimensional particle flow allowing recording from the side all particles with a high speed camera. The overall aim of this research is to measure the trajectories of all particles and to analyze the fluctuations of the solid discharge as well as the state of movement (rolling or saltation). First the trajectory of a single saltating or rolling particle was analyzed (Ancey et al. 2002; Ancey et al. 2003). Secondly, the aim was to measure the trajectories of all particles and to analyze the fluctuations of the solid discharge as well as the state of movement, rolling or saltation (Boehm et al. 2004; Boehm 2005; Boehm et al. 2006). More recently, spherical glass beads with a diameter of 4 mm together with 6 mm beads were also injected in the channel in order to study two-size mixtures. The first objective of this paper is to present the amendments made to the experimental procedure and image analysis algorithms, to be able to process two-size mixtures. With the help of a preliminary experiment, the second objective is to compare the two-diameter mixture bed load flow to the uniform bead case.

2 EXPERIMENTAL FACILITIES AND TECHNIQUES

Experiments were carried out in a tilted, narrow, glass-sided channel, 2 m in length. Figure 1 shows a sketch of the experimental facility. The channel width W was adjusted to 6.5 mm. The particle diameters were 4 and 6 mm; Even with the 4 mm beads, the particle motion remained approximately two-dimensional and stayed therefore in the focal plane of the camera. The channel slope $\tan\theta$ ranged from 7.5% to 12.5% for the experiments presented in this paper. The channel base consisted of half-

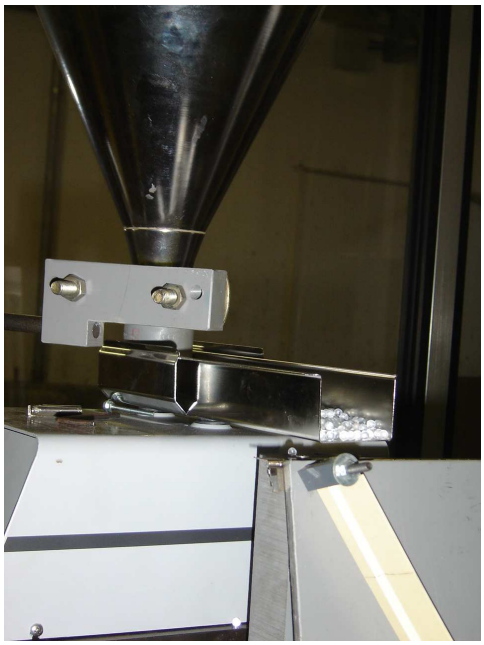

Figure 2: photo of the second reservoir

cylinders of equal size ($r = 3$ mm), but they were randomly arranged on different levels, from 0 to 5.5 mm, by increments of 0.5 mm. These levels were generated using a sequence of uniformly distributed random numbers.

An obstacle was set at the channel outlet to enable bed formation and prevent full bed erosion; its height could be adjusted. The procedure used for building the bed is explained in Sec. 2.3.

2.1 *Solid and water supplies*

Black spherical glass beads with a nominal diameter d of 6 mm (provided by Sigmund Lindner GmbH, Germany) and transparent spherical glass beads of 4 mm (provided by Cimap, France) both with a density ρ_p of 2500 kg/m^3 were used. The black beads were in-

Table 1: Flow characteristics and time-averaged values of dimensionless numbers characterizing bed load and water flow. E12-16 is the unimodal case and G12-10-19, the two-size mixture case.

Experiment	E12-16	G12-10-19
$\tan\theta$ (%)	12.5	12.5
$\dot{n}$ (beads/s)	15.5	9.9(6mm)+18.9(4mm)
q_s (10^{-3} m^2/s)	0.27	0.27
q_w (10^{-3} m^2/s)	3.85	7.66
C_s (%)	7.0	3.5
$h\,(mm)$	8.2	15.2
u_f (m/s)	0.47	0.50
Re	4360	5398
Fr	2.09	1.31
h/d	1.4	3.0
$2h/W$	2.5	4.7

jected from a reservoir into the channel using a wheel driven by a direct current motor and equipped with 20 hollows on the circumference.The transparent beads were injected with a second reservoir as depicted in Figure 2. The base of the machine was made of a vibrating device allowing the beads to fall 5 by 5 on a ramp leading to the channel inlet. For the uniform bead experiments presented here, the injection rate $\dot{n}$ ranged from 5 to 26 beads per second, with an uncertainty of less than 5%. For the two-size mixture, The injection rates were 9.9 beads per seconds for the 6 mm beads and 18.9 beads per seconds for the 4 mm beads with an uncertainty on of 15% on the 4 mm beads. This corresponded to a volumic solid discharge per unit width q_s of $7 - 76 \times 10^{-5}$ m^2/s (9.7×10^{-5} m^2/s for the transparent beads). The water supply at the channel entrance was controlled by an electromagnetic flow meter provided by Krohne (France). The discharge per unit width q_w ranged from 3 to 15×10^{-3} m^2/s (7.6×10^{-3} m^2/s for the two-size mixture). Parameters relative to the unimodal case E12-16 and the two-diameter case G12-10-19 are summarized in table 1. Those two experiments at the same slope 12.5% were chosen for comparison because they had the same volumic solid discharge.

2.2 *Dimensionless numbers*

The hydraulic conditions can be specified using classic dimensionless numbers. In table 1, h is the time-averaged flow depth. The flow Reynolds number is defined as $\mathrm{Re} = 4R_h\bar{u}_f/\nu$, where $R_h = Wh/(2h + W)$ denotes hydraulic radius, $\bar{u}_f = q_w/h$ fluid velocity (averaged in the y- and z-directions), ν kinematic viscosity of water. The Froude number $\mathrm{Fr} = \bar{u}_f/\sqrt{gh}$ (where g denotes gravity acceleration) varied significantly over the experiment duration and along the main stream direction. The mean Fr values are reported.

The solid concentration is defined as the ratio of the solid and the water discharge $C_s = q_s/q_w$.

Note that the dimensionless number values differ substantially from the values usually found in the hydraulics literature. The reason is twofold: first we used a short and narrow channel, which led to studying low Reynolds number regimes, whereas in most experiments on bed load transport, one takes care to avoid such regimes; this is the price to pay to have access to the details of particle movements. Since we used coarse particles, particle motion was weakly dependent on the actual value of the flow Reynolds number and turbulence structure. Therefore we think that the small size of the experimental setup is not a handicap. Second we mostly studied supercritical flows because of the steep slopes investigated. However, in a supercritical regime, flow depth was low: on the order of the particle size, meaning that particle motion could be affected by the water free surface.

2.3 *Experimental procedures*

We present here the procedure used to reach equilibrium with the two-size mixture. The preliminary procedure can be split into three major steps. First of all, a particle bed was built along the channel base, which remained stationary on average. To that end, an equilibrium between the water discharge, solid discharge, bed elevation, and channel slope was sought. This equilibrium was reached by using the following procedure:

1. The water discharge was set to a constant value.

2. An obstacle was positioned at the downstream end of the channel. The solid discharges at the channel entrance were set to a constant value. The channel was initially empty with only the steel bottom. The bed was built progressively by injecting the 4 mm beads and the 6 mm beads. The 6 mm beads represented 34% of the total number of beads but 64% of the total solid discharge (factor 3.375 between masses). The solid discharge per unit width q_s was calculated by the relation $q_s = \pi d^3\dot{n}/(6W)$. The first beads supplied by the feeding system were stopped by the obstacle at the channel outlet and started to form a bed. The bed line rose to the level of the obstacle and beads began to leave the channel. After approximately 10 minutes, the system arrived at bed load equilibrium, i.e., there was no more bed degradation nor aggradation over a sufficiently long time interval.

3. In order to make the bed line parallel with the channel base, the water discharge was then adjusted. After several iterations, we arrived at the

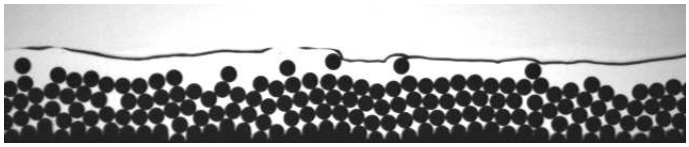

Figure 3: image corresponding to the unimodal case E12-16 with 6 mm beads, $\tan\theta = 12.5\%$

configuration with the bed line slope matching the channel base inclination. Average equilibrium conditions were sustained over long time periods, basically as long as 30 minutes.

Once bed equilibrium was reached, the particles and the water stream were filmed using a Pulnix partial scan video camera (progressive scan TM-6705AN). The camera was placed perpendicular to the glass panes at a distance of 115 cm from the channel, approximately 80 cm upstream from the channel outlet. It was inclined at the same angle as the channel. Lights were positioned in the backside of the channel. A new high bright white LED backligt device provided by Phlox was used especially for the detection of the 4 mm transparent beads to ensure an uniform and stable lighting. An area of approximately 25 cm in length and 8 cm in height was filmed and later reduced to accelerate image processing.

The camera resolution was 640×192 pixels for a frame rate of $f = 129.2$ fps (exposure time: 0.2 ms, 256 gray levels). Each sequence was limited to 8000 images due to limited computer memory; this corresponded to an observation duration of approximately 1 minute.

Each experiment was repeated at least twice in order to spot possible experimental problems and to get an idea of the data scattering.

2.4 *Image processing*

Images were analyzed using the WIMA software, provided by the *Traitement du Signal et Instrumentation* laboratory in Saint-Etienne (France). Positions of the 6 mm bead mass centers were detected by means of several algorithms comparing the filmed images with the image of a model bead and calculating the correlation maxima to obtain the bead positions. For the 4 mm beads, other algorithms combining gaussian filtering, reconstruction by conditional dilatation and several morphological operations were used to determine the positions of the beads.

2.5 *Data processing*

Data obtained from the image sequences were analyzed to obtain the particle trajectories. For this purpose, we developed a particle-tracking algorithm combining both the 4 mm and 6 mm bead detections. This algorithm stemmed from the initial tracking procedure developed by (Boehm et al. 2006). This algorithm compared the bead positions of two consecutive images to determine the trajectory of each bead step by step. Since the particle movement was nearly two-dimensional (even for 4 mm beads) and the displacement of a particle between two images was always smaller than a particle diameter, the trajectories (approximately 13000 per sequence) could be calculated with no significant error. The state of movement of a particle was also defined by considering that each bead was always either in a resting, rolling, or saltating regime. A bead was declared in saltation when no other beads were found in its neighborhood (Boehm et al. 2004). Since the experiments involved a mobile bed, the water depth was defined as the difference between the free surface and the bed surface elevation. The water free surface (averaged in the direction perpendicular to the channel walls) was detected using its slim form; missing portions were inter- or extrapolated. The bed surface profile was taken as the line linking the top points of the uppermost resting or rolling beads.

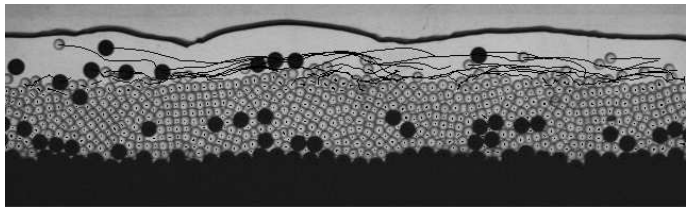

Figure 4: 30th image of the two-size mixture G12-10-19 with superimposed trajectories corresponding to the first 30 images

3 RESULTS

3.1 *Water depth and solid transport concentration*

Contrary to the 6 mm-bead uniform case which movement was perfectly two-dimensional (Figure 3) 4 mm beads in the 6.5 mm channel exhibited a strong tendency to blockage because of the ratio 4 mm compared to 6.5 mm. When equilibrium was reached, the bed was mainly formed by less mobile 4 mm beads (Figure 4). As a result, flow resistance was greater with 4 mm beads generating a higher water depth. For the same solid discharge, it was necessary to input a water discharge twice as much as in the unimodal case meaning that the concentration C_s was divided by a factor 2. Of course a higher water depth also meant more dissipation on the transparent walls of the flume. However the use of a Einstein type side wall correction as described in (Frey et al. 2006) still resulted in bed resistance coefficients higher with two-size mixtures than with 6 mm beads. In our case the imbricated structure of the two-size mixture had a stronger effect than the lower h/d ratio.

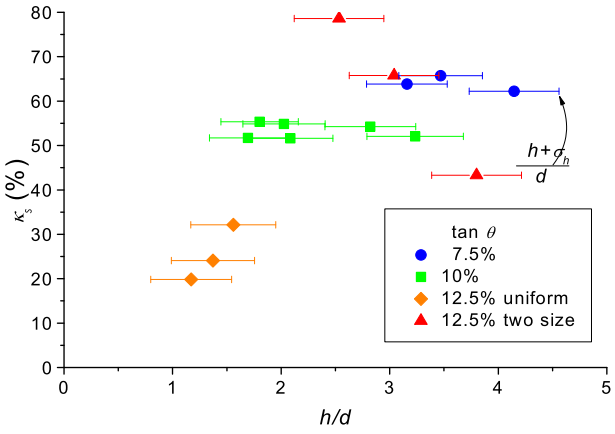

Figure 5: Relative contribution of the saltating particles to the solid discharge κ_s as a function of the ratio h/d, where h and d are the water depth and the particle diameter, respectively. The error bars represent the standard deviation $(h \pm \sigma_h)/d$ (Boehm 2005).

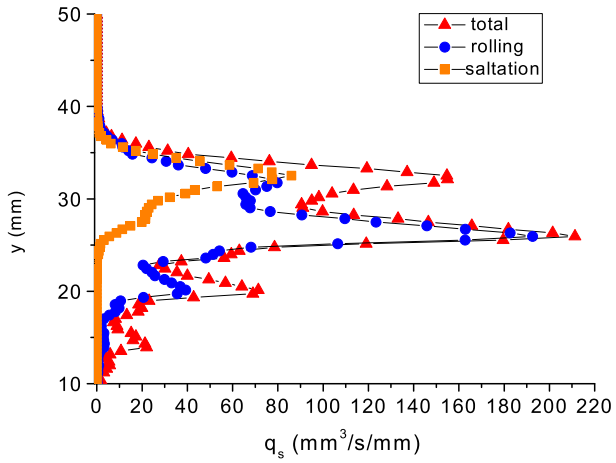

Figure 6: Solid discharge q_s as a function of the y vertical coordinate (total solid discharge and elementary contributions) for E12-16.

3.2 *Contribution of the saltating regime to the solid discharge*

We broke down the solid discharge into the contributions due to the saltating and the rolling beads. We introduced κ_s as the ratio of the volume flow rate due to the saltating particles to the total solid discharge.

When working with uniform beads (Boehm 2005) at constant slope (tests were made for $\tan\theta = 10\%$), there was almost no variation in the ratio κ_s with total solid discharge. In contrast, this ratio turned out to be strongly dependent on channel slope and water depth h. This dependence can be shown by plotting κ_s as a function of h/d for the different slopes (see Figure 5). For $\tan\theta = 7.5\%$, κ_s was higher, but still constant. It was then concluded that for mild slopes (7.5 and 10%), κ_s was a function of $\tan\theta$ only. For a steeper slope though (12.5%), the diagram shows that κ_s was a function of h/d.

For $\tan\theta = 12.5\%$ in the uniform case (E12-16), beads in saltation got in touch with the water free surface quite frequently, which implied that their vertical motion was hindered by the low water depth. This might explain why saltation was impeded here, many particles had to be transported in the rolling motion, which occupied less space in the vertical direction.

On the opposite, for the experiments made at milder slopes $\tan\theta = 7.5$ and 10%, the particle leap height was only slightly influenced by the water line. In that case, we would have expected that the ratio κ_s could freely adapt and vary with slope and solid discharge and/or the relative submersion, but it turned out that it depended on the channel slope alone.

In the same way, we plotted the two-size experiment G12-10-19 on the same figure 5. Three points were added (triangles) corresponding to the 6 mm fraction (κ_s about 80%), the 4 mm fraction (κ_s about 43%) and the two-size mixture (κ_s about 66 %). These proportions confirm our first impressions when visualizing images, that is a bed line mainly formed of 4 mm beads with very few 6 mm black beads in the rolling regime resulting in a high proportion of saltating discharge. More surprisingly is that the proportion of saltating discharge for the two-size mixture G12-10-19 at a slope of 12.5% and h/d of 3 has about the same value as for runs performed on a slope of 7.5% with the same value of h/d. By contrast for the uniform case E12-16 on a slope of 12.5%, κ_s was much lower but with a h/d value close to 1. It implies that there is no dependency on slope but rather on h/d and that the proportion of rolling and saltating beads is highly sensitive to the free surface as was already noted in the uniform case.

3.3 *solid discharge vertical profiles*

The distributions of q_s along the vertical together with the contributions of saltation and rolling to the total solid discharge are plotted for the unimodal E12-16 experiment (Figure 6) and the G12-10-19 two-size experiment (Figure 7) respectively. It is to be noted that the contribution of resting beads was not equal to zero because of vibration resulting of low movement not considered as rolling. Therefore the total solid discharge on Figure 6 may be higher than the added contributions of rolling and saltation.

Figure 6 shows three peaks at intervals of approximately one particle diameter corresponding to three peaks of rolling. There is only one peak for saltation approximately equal to the uppermost rolling peak at the same location (y= 32 mm), adding to-

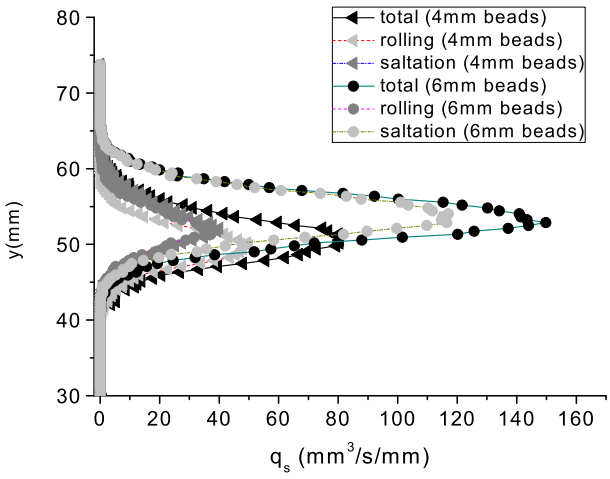

Figure 7: Solid discharge q_s as a function of the y vertical coordinate (total solid discharge and elementary contributions) for G12-10-19.

gether to form the uppermost total peak. This profile thus clearly indicates that the particle bed had a layered structure and that the two uppermost bed layers (y= 20 mm and 26 mm) were prone to rolling.

On Figure 7 the same distributions are broken down according to the size fraction. There is also only one peak of saltation for the two types of particles. By contrast to the unimodal case there is only one rolling peak at a slightly lower position than the saltation peak. It indicates that the collective motion of rolling particles was only possible on the layer near to the bed surface. As already described, the 4 mm beads formed an imbricated bed preventing movement of the bed layers.

4 CONCLUSIONS

In this paper, we investigated the bed load sediment transport of a two-size mixture (4 mm and 6 mm beads) using an idealized experimental setup and we compared this case with previous results obtained with uniform beads (6 mm) in the same flume. Since the 4 mm beads in the 6.5 mm wide channel exhibited a strong tendency to blockage, when equilibrium was reached, the bed was mainly formed by imbricated 4 mm beads. As a result, we observed a number of interesting properties:

- it was necessary to input a water discharge twice as much as in the unimodal case meaning that the concentration C_s was divided by a factor 2 and the water depth much higher. In our case the imbricated structure of the two-size mixture had a stronger effect than the lower h/d ratio.

- We broke down the volumic solid discharge into the contributions due to the saltating and the rolling beads for comparison with previous uniform results. the proportion of saltating discharge for the two-size mixture G12-10-19 at a slope of 12.5% and h/d of 3 displayed about the same value as uniform runs performed on a slope of 7.5% with about the same value of h/d. By contrast for the uniform case E12-16 on a slope of 12.5% and a h/d value close to 1, the proportion of saltating discharge was much lower. It implies that there is no dependency on slope but rather on h/d and that the proportion of rolling and saltating beads is highly sensitive to the free surface as was already noted in the uniform case.

- The distributions of q_s along the vertical together with the contributions of saltation and rolling to the total solid discharge showed very different patterns depending on the uniform case and the two-size mixture. In the uniform case, three peaks of rolling could be distinguished at intervals of about one particle diameter indicating a rather loose bed packing allowing the movement of beads in the uppermost bed layers. By contrast to the unimodal case there was only one rolling peak indicating that the 4 mm beads formed an imbricated bed preventing movement of the bed layers.

Results presented in this paper confirm that the free surface acting as a physical barrier by truncating the saltation trajectories is of the utmost importance on steep slopes. Further experiments are under way to better understand bedload sediment transport with a two-size mixture and particularly to investigate the effect of the bed history and structure.

ACKNOWLEDGMENTS

This study was supported by Cemagref and by the program ECCO/PNRH of ANR and INSU (ANR-05-ECCO-015).

REFERENCES

Ancey, C., F. Bigillon, P. Frey, and R. Ducret (2003). Rolling motion of a bead in a rapid water stream. *Phys. Rev. E 67*, 011303.

Ancey, C., F. Bigillon, P. Frey, R. Ducret, and J. Lanier (2002). Saltating motion of a bead in a rapid water stream. *Phys. Rev. E 66*, 036306.

Barry, J., J. Buffington, and J. King (2004). A general power equation for predicting bed load transport rates in gravel bed rivers. *Water Resour. Res. 40*, W10401.

Boehm, T. (2005). *Motion and interaction of a set of particles in a supercritical flow*. Ph. D. thesis, Joseph Fourier University, Grenoble, 172.

Boehm, T., C. Ancey, P. Frey, J.-L. Reboud, and C. Ducottet (2004). Fluctuations of the solid discharge of gravity-driven particle flows in a turbulent stream. *Phys. Rev. E 69*, 061307.

Boehm, T., P. Frey, C. Ducottet, C. Ancey, M. Jodeau, and J.-L. Reboud (2006). Two-dimensional motion of a set of particles in a free surface flow with image processing. *Experiments in Fluids 41*, 1–11.

Frey, P., M. Dufresne, T. Boehm, M. Jodeau, and C. Ancey (2006). Experimental study of bed load on steep slopes. In *River flow, Int. Conf. on Fluvial Hydraulics*, Lisbonne, 6-8 september, pp. 887–893. Balkema.

Martin, Y. (2003). Evaluation of bed load transport formulae using field evidence from the Vedder River, British Columbia. *Geomorphology 53*, 75–95.

Wilcock, P. (2001). Toward a practical method for estimating sediment-transport rates in gravel bed-rivers. *Earth Surface Processes and Landforms 26*, 1395–1408.